Available online at www.sciencedirect.com
SCIENCE DIRECT®
Journal of Sound and Vibration 278 (2004) 413–436
JOURNAL OF SOUND AND VIBRATION
www.elsevier.com/locate/jsvi

Development of an energy boundary element formulation for computing high-frequency sound radiation from incoherent intensity boundary conditions

A. Wang[a], N. Vlahopoulos[a,*], K. Wu[b]

[a] *Department of Naval Architecture and Marine Engineering, University of Michigan, 2600 Draper Road, Ann Arbor, MI 48109-2145, USA*
[b] *Department E46, Signatures and hydrodynamics, Newport News Shipbuilding, 4101 Washington Av., Newport News, VA 23609-2770, USA*

Received 18 November 2002; accepted 19 June 2004

Abstract

An energy boundary element analysis (EBEA) formulation is presented for calculating sound radiation at high frequency from a radiator with arbitrary shape. The EBEA development presented in this paper compliments previous energy finite-element analysis (EFEA) developments for computing high-frequency vibration of structures immersed in an acoustic medium. From the EFEA solution the structural vibrational energy throughout the structure and the acoustic power radiated from each surface element in contact with the surrounding fluid are computed. The EBEA utilizes the information for the acoustic power radiated from each element of the outer surface of the structure as a boundary condition in order to compute the acoustic field in an unbound medium with no damping that surrounds the radiating structure. Since the structural vibration between different elements is considered as incoherent in the EFEA, the acoustic intensity associated with each surface element that radiates in the surrounding medium is also considered as incoherent between different elements in the EBEA formulation. The governing integral equation of EBEA is established, and a numerical solution is presented. The present method is validated by comparing EBEA results to analytical solutions and to numerical results from an axi-symmetric *hp* finite-element code with infinite acoustic elements suitable for structural acoustic computations. Good correlation is demonstrated for all the analyses.

*Corresponding author. Tel.: +1-734-764-8341; fax: +1-734-936-8820.
E-mail address: nickvl@engin.umich.edu (N. Vlahopoulos).

0022-460X/$ - see front matter © 2003 Elsevier Ltd. All rights reserved.
doi:10.1016/j.jsv.2003.06.018

1. Introduction

A new energy boundary element analysis (EBEA) formulation for computing the noise radiated from a vibrating structure at high frequencies is presented in this paper. The vibrational energy of the structure is considered to be calculated by the energy finite-element analysis (EFEA) [1–7]. The EFEA constitutes a recent development for computing high-frequency vibration and offers an attractive alternative to the traditional statistical energy analysis (SEA) approach [8]. The developments of the primary variables and of the main system of equations in SEA are based on a modal approach, while the definitions of the primary variables and of the governing differential equations in EFEA are based on a wave approach [3]. Both formulations are commonly employing wave methods for estimating coupling loss factors (SEA) and power transfer coefficients (EFEA) [9]. In SEA the primary variables are defined as the frequency averaged over a one-third octave band energy stored in each group of similar modes. In EFEA the primary variables are comprised by the space averaged over a wavelength and frequency averaged over a one-third octave band energy density. Both methods can also compute the high-frequency acoustic field generated from the structural vibration inside a dissipative, reverberant, and fully enclosed acoustic space. The interior acoustic field is modelled by the SEA as a group of orthogonal incoherent interior acoustic normal modes, and by the EFEA as an incoherent summation of a three-dimensional orthogonal basis of waves. In both methods the amount of the structural vibrational energy converted into incoherent acoustic intensity constitutes the boundary condition for the high-frequency acoustic analysis. When an exterior acoustic medium is considered, the influence of the external fluid on the structural vibration is accounted in both formulations through the effective mass effect and the radiation damping. The radiation efficiency employed in the SEA and the EFEA vibration analyses determines the amount of acoustic power radiated in the fluid from the structural vibration. The total amount of the radiated acoustic power can be computed in SEA by summarizing the acoustic power radiated in the fluid by all the structural subsystems in contact with the surrounding acoustic medium. Similarly, in EFEA the total acoustic power can be determined by integrating the acoustic intensity over all the structural elements which are in contact with the fluid. Both methods can compute the total radiated power. However, neither one of the two methods is applicable for computing the acoustic field generated at the specific field points around the structure since an orthogonal modal basis or wave basis cannot be defined for the unbound medium. Also in both SEA and EFEA, acoustic damping must be assigned to the acoustic medium; this is not the case in the radiation solution considered in this paper. However, for field points which are far enough from the radiator so that the radiating object can be approximated by a point source, the acoustic energy and the acoustic intensity can be computed from the analytical equations of a single point source located at the center of the radiating object and emitting acoustic power equal to the total acoustic power emitted by the radiator.

The EBEA formulation presented in this paper is meant to utilize the results from the EFEA computations in order to calculate the acoustic field radiated from a vibrating structure immersed in an unbound acoustic medium without damping. From the structural EFEA analysis, the acoustic power radiated from each structural element of the EFEA model in the surrounding fluid is computed. Since the vibrational field in the EFEA is considered as reverberant, the vibrational energy in the structural elements and the acoustic intensity radiated from the structural elements in contact with the fluid are incoherent among different elements. The incoherent acoustic

intensity on the interface between a structure and an acoustic cavity has been employed in the past as a boundary condition in high-frequency SEA and EFEA interior acoustic computations [4,8]. Similarly, the incoherent acoustic intensities radiated in the unbound medium from each element on the outer surface of a structure comprise the boundary conditions for the EBEA computations.

The concept of employing boundary elements for high-frequency analyses has been introduced in the past [10–14]. In Refs. [10,14] a linear superposition principle and the Huygens Principle were employed for deriving integral equations for the energy quantities of the wave fields inside a plate or inside an acoustic enclosure. The energy field variables were considered as the superposition of the direct field created by primary sources inside the domain and a diffracted field created by secondary sources. The distributions of secondary sources on the boundary of the domain were computed first using a collection approach which enforces a power balance on the boundary of the domain. Once the strengths of the secondary sources were computed, the energy variables for the field were evaluated based on boundary element integrals. An ensemble averaging operator was applied on the integral equations in order to eliminate the interferences between the secondary sources. Numerical simulations were performed for the vibrational energy of a pair of co-linear plates with different flexural rigidities and for the acoustic field generated by a point inside an enclosure. In Ref. [11] an indirect boundary element formulation was presented for a coupled high-frequency structural–acoustic analysis. The energy finite element method for the structure and an acoustic energy boundary element method for the interior acoustic space were combined in a coupled solution. Acoustic energy sources were distributed on the surface of the acoustic cavity and expressions were developed for linking the acoustic energy in the interior field with the surface acoustic energy sources. Joint matrices were formulated between the structural energy variables and the acoustic energy variables for developing a coupled structural–acoustic solution suitable for solving systems of plates interacting with interior acoustic spaces. In Ref. [12] a boundary element method for high-frequency acoustic analysis of interior acoustic spaces was presented. A collocation boundary element approach was utilized for solving numerically the governing differential equations for the acoustic energy density of an acoustic cavity. Finally, a direct boundary element formulation was presented in Ref. [13] for the dynamic analysis of eleastic, homogeneous rods and beams subjected to high-frequency harmonic loadings.

In the conventional boundary element method (BEM) for acoustic radiation [15–25] the acoustic pressure and the acoustic velocity on the surface of the model comprise the primary variables. In BEM the relative phase information between the primary variables is important for the solution, and analyses are performed at distinct frequencies. The governing integral equation of the conventional BEM provides the starting point for deriving the EBEA governing integral equation. The phase dependent primary variables of the BEM formulation are converted into the incoherent acoustic intensity boundary conditions by applying an ensemble averaging operator [10,14,26,27] on the BEM integral equations. Since ensemble averaging is assumed as equivalent to frequency averaging in high-frequency analysis [5,8,10,14,28–30], the EBEA governing integral equations for the frequency averaged acoustic quantities are assumed to be equivalent for the equations that are developed through ensemble averaging. A numerical solution to the EBEA governing integral equation is obtained by distributing incoherent energy sources or sinks on the individual elements of the EBEA model [10–12,14]. The acoustic power radiated from each element, computed by the EFEA, constitutes the boundary conditions for the EBEA. The magnitudes of the energy sources and sinks are computed from a set of equations stating that the combined effect of all the energy

sources and sinks distributed on each element must satisfy the prescribed intensity boundary conditions on the surface of the radiator. This approach is similar to the source panel method [31] in potential flows where a distribution of flow sources or sinks is placed on the surface of an object and their strengths are evaluated by satisfying a set of known normal velocity boundary conditions. It is also similar to the EBEA methods presented for interior acoustic calculations in Ref. [10–12,14]. However, the purpose of the EBEA presented in this paper is to calculate the frequency averaged acoustic energy density and the frequency averaged acoustic intensity in the exterior acoustic domain without dissipation at high frequency, when the incoherent frequency averaged normal acoustic intensity on the surface of the radiator is evaluated from an EFEA analysis. For field points that are not far enough from the radiating structure in order to approximate the radiator as a single point source, the EBEA provides better results. Since the EBEA does not capture phase information the number of elements is not dictated by the frequency of analysis as in the conventional BEM, thus the number of required elements does not increase with frequency. However, the EBEA is only meaningful at high frequencies where the phase information can be neglected since the acoustic field is considered as incoherent. The boundary conditions in the EBEA are defined in terms of surface intensity while either a pressure, a velocity, an impedance, or a mixed boundary condition is defined in the BEM. Finally, the EBEA does not present any singularities associated with irregular frequencies as it happens in the traditional BEM.

In Section 2, the integral equations for the EBEA are established. The corresponding Green functions are obtained from these integral formulas. The numerical implementation of the EBEA is derived in Section 3. A discussion on how a second order singularity is avoided during the evaluation of the integrals of the diagonal terms in the numerical implementation is presented. Finally, the reason that a non-uniqueness issue is not present in the EBEA formulation is also discussed. The validity of the EBEA formulation and its numerical implementation is demonstrated in Section 4 by comparing EBEA results to analytical solutions for exterior radiation in an unbound acoustic medium without dissipation, and by comparing EBEA results to numerical solutions obtained from a very dense axi-symmetric, *hp* finite-element model, with infinite acoustic elements [32].

2. Theoretical formulation

Two energy quantities are computed in the EBEA formulation, the frequency-averaged acoustic energy density, and the frequency-averaged acoustic intensity. The basic assumption in deriving the EBEA formulation is that the energy sources on each element are incoherent among different elements [10,11,14]. This assumption is in-line with the existing high-frequency SEA and EFEA formulations, and it is also necessary in order to utilize the incoherent acoustic power computed by the EFEA analysis on the outer part of a structure as a boundary condition for predicting the radiated acoustic field [33].

2.1. Characteristics of incoherent sources

Considering two elementary sources with the complex strength amplitudes of A_i and A_j, respectively, the source cross-spectral density (CSD), which is used to express the interdependence

relationship between these two sources, is [14,26,27]

$$\Gamma_{ij}(\omega) = E[A_i^*(\omega)A_j(\omega)], \tag{1}$$

where ω is the circular frequency, the notation $E[\cdot]$ denotes the ensemble averaging and $(\,)^*$ indicates the conjugate of a complex number. The ensemble averaging operator $E[\cdot]$ is introduced as

$$E[A_i(\omega)A_j^*(\omega)] = \begin{cases} |A_i(\omega)|^2, & i = j, \\ 0, & i \neq j. \end{cases} \tag{2}$$

Then, the coherence function between source amplitudes can be defined similar to Ref. [27]:

$$\gamma_{ij}^2(\omega) = \frac{|\Gamma_{ij}(\omega)|^2}{\Gamma_{ii}(\omega)\Gamma_{jj}(\omega)}, \tag{3}$$

where $0 \leqslant \gamma_{ij}^2 \leqslant 1$ and $\Gamma_{ii}(\omega)$ and $\Gamma_{ij}(\omega)$ are, respectively, the auto- and CSD functions of the source. The matrix γ_{ij}^2 represents the coherence between sources. For incoherent sources, the coherence matrix becomes the identity matrix and the cross terms are zero, or

$$\gamma_{ij}^2 = \begin{cases} 1, & i = j, \\ 0, & i \neq j. \end{cases} \tag{4}$$

In the high-frequency methods the frequency averaging is considered as equivalent with the ensemble averaging [5,8,14,28–30] since the variation in the wavelengths induced by the differences in frequency is equivalent to the variation in the sources at a single frequency. Therefore, the ensemble averaged acoustic quantities developed by applying the operator $E[\cdot]$ to the boundary element integral equations are equivalent to acoustic quantities that are frequency averaged over a one-third octave band which is the typical frequency averaging range in SEA and EFEA applications.

2.2. Integral equations for the EBEA

The EBEA formulation is developed from the integral formulas for the acoustic pressure or velocity of the conventional BEM. First, the time averaged over a period acoustic energy density at a field point Y is expressed in terms of the acoustic velocity and the acoustic pressure as [11,34]

$$\langle e_Y \rangle = \frac{1}{4}\left[\rho \hat{\mathbf{v}}_Y \cdot \hat{\mathbf{v}}_Y^* + \frac{1}{\rho c^2}\hat{p}_Y \hat{p}_Y^*\right], \tag{5}$$

where ρ is the density of the acoustic medium, c is the speed of the sound in the medium, $\hat{\mathbf{v}}$ and $\hat{p}$ are the acoustic velocity and the acoustic pressure, respectively, $\langle\rangle$ indicates time averaging over a period (i.e., $\langle A \rangle = (1/T)\int_t^{t+T} A(\tau)\,\mathrm{d}\tau$), and symbol $\hat{}$ indicates complex quantities. The time averaged over a period acoustic intensity can also be written as [11,34]

$$\langle \mathbf{I}_Y \rangle = \tfrac{1}{2}\mathrm{Re}(\hat{p}_Y \hat{\mathbf{v}}_Y^*). \tag{6}$$

In order to develop the primary variables of the EBEA, the ensemble averaging operator [14,27] is applied to the equations for $\langle e_Y \rangle$ and $\langle \mathbf{I}_Y \rangle$ resulting in

$$\tilde{e}_Y = E[\langle e_Y \rangle] = \frac{1}{4}\left[\rho E[\hat{\mathbf{v}}_Y \cdot \hat{\mathbf{v}}_Y^*] + \frac{1}{\rho c^2} E[\hat{p}_Y \hat{p}_Y^*]\right] \tag{7}$$

and

$$\tilde{\mathbf{I}}_Y = E[\langle \mathbf{I}_Y \rangle] = \tfrac{1}{2}\mathrm{Re}(E[\hat{p}_Y \hat{\mathbf{v}}_Y^*]), \tag{8}$$

since the ensemble averaging in the high-frequency methods is considered as equivalent to frequency averaging, $\tilde{e}_Y$ and $\tilde{\mathbf{I}}_Y$ represent the time averaged over a period and frequency averaged over one-third octave band energy density and intensity at a field point Y.

In the conventional indirect boundary integral method, the acoustic pressure at any field point Y exterior to the structure is expressed as [15,16]

$$\hat{p}_Y = \int_S A(P) g(P, Y)\, \mathrm{d}S, \tag{9}$$

where S is the surface of the structure, P denotes the point located on the surface S, $A(P)$ is the complex source strength amplitude at P, and $g(P, Y) = \mathrm{e}^{-\mathrm{i}kr}/(4\pi r)$ is the Green function for three-dimensional infinite system, r is the distance between points P and Y, and k is the wave number. The same Green's function has been utilized in previous EBEA formulations presented for interior acoustics [10–12,14] and it originates from the conventional BEA formulations for acoustics [18]. The acoustical velocity vector can be obtained from the acoustic pressure

$$\hat{\mathbf{v}}_Y = -\frac{1}{\mathrm{i}\omega\rho}\nabla\hat{p}_Y = -\frac{1}{\mathrm{i}\omega\rho}\int_S A \nabla g(P, Y)\, \mathrm{d}S, \tag{10}$$

where

$$\nabla g(P, Y) = -\frac{1}{4\pi r^2}(1 + \mathrm{i}kr)\mathrm{e}^{-\mathrm{i}kr}\mathbf{E}_r, \tag{11}$$

and where $\mathbf{E}_r$ denotes the unit vector from P to Y.

Eqs. (9) and (10) are employed for developing expressions for the ensemble averaged quantities $E[\hat{p}_Y \hat{p}_Y^*]$, $E[\hat{\mathbf{v}}_Y \cdot \hat{\mathbf{v}}_Y^*]$ and $E[\hat{p}_Y \hat{\mathbf{v}}_Y^*]$. The latter expressions are introduced in Eqs. (7) and (8) in order to develop the equations for the primary variables of the EBEA formulation. The acoustic pressure square is calculated as

$$\begin{aligned} \hat{p}_Y \hat{p}_Y^* &= \int_S A(P') g(P', Y)\, \mathrm{d}S \int_S A^*(P'') g^*(P'', Y)\, \mathrm{d}S \\ &= \int_S \int_S A(P') A^*(P'') g(P', Y) g^*(P'', Y)\, \mathrm{d}S'\, \mathrm{d}S''. \end{aligned} \tag{12}$$

By applying the ensemble averaging on both sides of the above equation results in

$$E[\hat{p}_Y \hat{p}_Y^*] = \int_S \int_S E[A(P') A^*(P'') g(P', Y) g^*(P'', Y)]\, \mathrm{d}S'\, \mathrm{d}S''. \tag{13}$$

Since the Green functions $g(P', Y)$ and $g(P'', Y)$ are deterministic variables, Eq. (13) reduces to

$$E[\hat{p}_Y \hat{p}_Y^*] = \int_S \int_S E[A(P')A^*(P'')]g(P', Y)g^*(P'', Y)\,\mathrm{d}S'\,\mathrm{d}S''. \tag{14}$$

According to Eq. (2), for incoherent sources, $E[A(P')A^*(P'')]$ is non-zero only for $P' = P''$. Thus, only the terms due to the same point (P,P) are retained in the integral equations, resulting in

$$E[\hat{p}_Y \hat{p}_Y^*] = \int_S \mu(P)|A(P)|^2|g(P, Y)|^2\,\mathrm{d}S. \tag{15}$$

In Eq. (15) the double integral is reduced to a single integral due to the zero cross terms in $E[A(P')A^*(P'')]$. This approach was introduced in Ref. [14] for reducing the double integrals of the secondary sources to single integrals at the boundary, under the assumption that the interferences between secondary sources are neglected. The variable $\mu(P)$ appears in the equation in order to retain the proper units during the reduction from a double to a single integral, and $\mu(P)$ is equal with the differential area associated with the location P of the integration.

Following a similar process for $E[\hat{\mathbf{v}}_Y \cdot \hat{\mathbf{v}}_Y^*]$ and $E[\hat{p}_Y \hat{\mathbf{v}}_Y^*]$ results in

$$E[\hat{\mathbf{v}}_Y \cdot \hat{\mathbf{v}}_Y^*] = \frac{1}{\omega^2\rho^2}\int_S \mu(P)|A(P)|^2|\nabla g(P, Y)|^2\,\mathrm{d}S \tag{16}$$

and

$$E[\hat{p}_Y \hat{\mathbf{v}}_Y^*] = \frac{1}{\mathrm{i}\omega\rho}\int_S \mu(P)|A(P)|^2 g(P, Y)\nabla g^*(P, Y)\,\mathrm{d}S. \tag{17}$$

Substituting Eqs. (15) and (16) into Eq. (7), results in

$$\tilde{e}_Y = \frac{1}{4}\left[\frac{1}{\rho\omega^2}\int_S \mu(P)|A(P)|^2\left(\frac{1}{16\pi^2 r^4} + \frac{k^2}{16\pi^2 r^2}\right)\mathrm{d}S + \frac{1}{\rho c^2}\int_S \mu(P)|A(P)|^2\frac{1}{16\pi^2 r^2}\,\mathrm{d}S\right]. \tag{18}$$

Using the relationship $c = \omega/k$ [9,35] reduces Eq. (18) to

$$\tilde{e}_Y = \frac{1}{\rho^2\omega^2}\int_S \mu(P)|A(P)|^2\left(\frac{\rho}{64\pi^2 r^4} + \frac{k^2\rho}{32\pi^2 r^2}\right)\mathrm{d}S. \tag{19}$$

Similarly, substituting Eq. (17) into Eq. (8), results in

$$\tilde{\mathbf{I}}_Y = \frac{1}{\rho^2\omega^2}\int_S \mu(P)|A(P)|^2\frac{k^2\rho c}{32\pi^2 r^2}\mathbf{E}_r\,\mathrm{d}S. \tag{20}$$

In Eqs. (19) and (20), the term $1/\rho^2\omega^2$ is a frequency-dependent term. The strength density of an energy source or sink can be defined as the product between the frequency-dependent term and the term $\mu(P)|A(P)|^2$:

$$\sigma(P) = \frac{\mu(P)}{\rho^2\omega^2}|A(P)|^2, \tag{21}$$

where $\sigma(P)$ denotes the strength density of the energy source placed at point P of the surface of the model. Acoustic energy sources are used in Refs. [10,14] to define the distribution of the secondary sources on the boundary of an acoustic cavity in order to capture the total field generated due to an excitation from primary sources inside the cavity. They are also used in Ref. [11] in order to create the coupling between a structure and the interior acoustic response.

In this paper they are utilized for solving a different problem, namely computing the radiated noise in an unbound acoustic medium without damping once the radiated acoustic intensity from a source immersed into fluid is known from an EFEA analysis [33]. Thus, Eqs. (19) and (20) can be written in their final form as

$$\tilde{e}_Y = \int_S \sigma(P)\left(\frac{\rho}{64\pi^2 r^4} + \frac{k^2\rho}{32\pi^2 r^2}\right) \mathrm{d}S \tag{22}$$

and

$$\tilde{\mathbf{I}}_Y = \int_S \sigma(P)\frac{k^2\rho c}{32\pi^2 r^2}\,\mathbf{E}_r\,\mathrm{d}S. \tag{23}$$

Eqs. (22) and (23) constitute the basic integral equations of the EBEA formulation.

3. Numerical implementation

The EBEA numerical formulation for the time and frequency-averaged acoustic energy density and intensity in the radiated field (Eqs. (22) and (23)) is developed by placing a continuous distribution of incoherent infinitesimal energy sources on the surface of the radiator similar to Refs. [10–12,14].

3.1. Numerical system of equations

The surface S of the radiator (Fig. 1) is divided into n quadrilateral or triangular elements. Incoherent energy sources or sinks are distributed on every element. In this work, the source strength density $\sigma_j\,(j = 1, 2, \ldots, n)$ on each element is considered to be constant, similar to a traditional collocation boundary element approach in acoustics [15]. Eqs. (22) and (23) can be rewritten in the discrete form by considering $\sigma(P)$ as constant over each element "j" and equal to σ_j:

$$\tilde{e}_Y = \sum_{j=1}^{n}\left[\sigma_j \int_{S_j} G(\boldsymbol{\xi}, \mathbf{Y})\,\mathrm{d}S\right], \quad \tilde{\boldsymbol{I}}_Y = \sum_{j=1}^{n}\left[\sigma_j \int_{S_j} \mathbf{H}(\boldsymbol{\xi}, \mathbf{Y})\,\mathrm{d}S\right], \tag{24, 25}$$

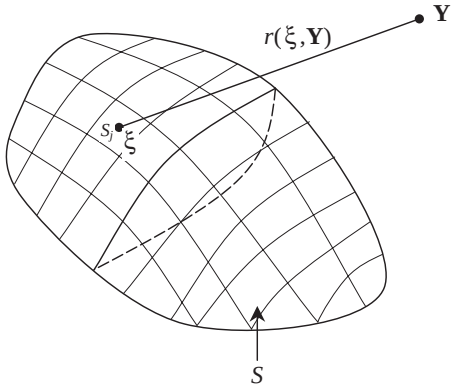

Fig. 1. Surface of an EBEA model divided into n quadrilaterals (or triangles).

where

$$G(\boldsymbol{\xi}, \mathbf{Y}) = \frac{\rho}{64\pi^2 r^4(\boldsymbol{\xi}, \mathbf{Y})} + \frac{k^2\rho}{32\pi^2 r^2(\boldsymbol{\xi}, \mathbf{Y})}$$

and

$$\mathbf{H}(\boldsymbol{\xi}, \mathbf{Y}) = \frac{k^2\rho c}{32\pi^2 r^2(\boldsymbol{\xi}, \mathbf{Y})}\mathbf{E}_r$$

are the Green functions for the time and frequency-averaged acoustic energy density and intensity in the free field, respectively, S_j indicates the surface of element j as shown in Fig. 1, and $\boldsymbol{\xi}$ is an arbitrary point on the element j. Since the source strength density σ_j is constant on each element, it can be factored outside the integral.

In order to develop the numerical system of equations that will allow to compute the values of the sources and sinks σ_j over the model, the field point Y is placed on an element q on the outer surface of the radiator and Eq. (25) provides the integral equation for the intensity $\tilde{\mathbf{I}}_Y$ on the element q. In order to avoid the singular integration within the element q in Eq. (25) the physical interpretation of the integral $\int_{S_q} \mathbf{H}(\boldsymbol{\xi}, \mathbf{Y})\,\mathrm{d}S$ is considered. This integral represents the acoustic intensity on element q generated by the source of element q itself. In order to avoid the computation of the singular integration the corresponding intensity is evaluated as half of the power of the element source divided by the element area. The averaged acoustic power radiated by element q itself is expressed as

$$P_q = \sigma_q A_q \frac{k^2\rho c}{8\pi}, \tag{26}$$

where σ_q is the source strength density on the element, and A_q is the area of element q. Half of this power is radiated from each side of the element, therefore the contribution from the element itself to the acoustic intensity at point Y located on element q is determined by

$$\tilde{\mathbf{I}}_q = \sigma_q \frac{k^2\rho c}{16\pi}\mathbf{n}_q, \tag{27}$$

where $\mathbf{n}_q$ is the outward unit normal vector of the element. Thus, Eq. (25) can be rewritten as

$$\tilde{\mathbf{I}}_Y = \sum_{j=1, j\neq q}^{n} \left[\sigma_j \int_{S_j} \mathbf{H}(\boldsymbol{\xi}, \mathbf{Y})\,\mathrm{d}S\right] + \sigma_q \frac{k^2\rho c}{16\pi}\mathbf{n}_q. \tag{28}$$

Since the radiated acoustic power from each element comprises the prescribed boundary condition, the time and frequency-averaged intensity on an element integrated over the area of the element must result into the prescribed radiated acoustic power:

$$\int_{S_i} \tilde{\mathbf{I}}_Y \cdot \mathbf{n}_i\,\mathrm{d}S = \bar{P}_i, \quad i = 1, 2, \ldots n, \tag{29}$$

where $\bar{P}_i$ is the prescribed radiated power from element i, and $\mathbf{n}_i$ is the normal (outward of the structure) vector of the element i. Substituting Eq. (28) in Eq. (29) results in

$$\bar{P}_i = \int_{S_i} \left\{ \sum_{j=1, j\neq i}^{n} \left[\sigma_j \int_{S_j} \mathbf{H}(\boldsymbol{\xi}, \boldsymbol{\eta}) \cdot \mathbf{n}_i\,\mathrm{d}S\right] + \sigma_i \frac{k^2\rho c}{16\pi} \right\} \mathrm{d}S, \quad i = 1, 2, \ldots, n, \tag{30}$$

where $\boldsymbol{\eta}$ and $\boldsymbol{\xi}$ are the arbitrary points in the elements i and j, respectively. By factoring outside the integral the strength of the energy sources or sinks distributed over each element, Eq. (30) is rewritten as

$$\bar{P}_i = \sum_{j=1, j\neq i}^{n} \left\{ \sigma_j \int_{S_i} \left[\int_{S_j} \mathbf{H}(\boldsymbol{\xi}, \boldsymbol{\eta}) \cdot \mathbf{n}_i \, \mathrm{d}S \right] \mathrm{d}S \right\} + \sigma_i A_i \frac{k^2 \rho c}{16\pi}, \quad i = 1, 2, \ldots, n, \tag{31}$$

where A_i is the area of the element i. Eq. (31) is written in the matrix form as

$$[K]\{\sigma\} = \{P\}, \tag{32}$$

where $\{P\}_{n\times 1} = \{\bar{P}_1 \ \bar{P}_2 \ \ldots \bar{P}_n\}^{\mathrm{T}}$ is the vector of prescribed boundary conditions, $\{\sigma\}_{n\times 1} = \{\sigma_1 \ \sigma_2 \ \ldots \ \sigma_n\}^{\mathrm{T}}$ is vector of the unknown variables and each term K_{ij} of the matrix $[K]$ is derived as

$$K_{ij} = \begin{cases} \int_{S_i} \left[\int_{S_j} \mathbf{H}(\boldsymbol{\xi}, \boldsymbol{\eta}) \cdot \mathbf{n}_i \, \mathrm{d}S \right] \mathrm{d}S, & i \neq j, \\ A_i \dfrac{k^2 \rho c}{16\pi}, & i = j. \end{cases} \tag{33}$$

The values of the acoustic energy sources or sinks are obtained by solving Eq. (32). Then by employing Eqs. (24) and (25), the time and frequency-averaged acoustic energy density and intensity can be determined at any field point within the acoustic medium exterior to the structure.

3.2. Numerical calculation

Eq. (32) is solved numerically. When i is not equal to j, the system matrix coefficient K_{ij} is calculated by a Gaussian quadrature as

$$K_{ij} = \sum_{k=1}^{n_g} \sum_{l=1}^{n_g} \left\{ \sum_{m=1}^{n_g} \sum_{n=1}^{n_g} \left[|J_{m,n}| \mathbf{H}(\xi_{m,n}, \eta_{k,l}) \cdot \mathbf{n}_i |J_{k,l}| W_m W_n W_k W_l \right] \right\}, \tag{34}$$

where n_g is the number of the Gaussian integration points for one-dimensional integral, $\xi_{m,n}$ and $\eta_{k,l}$ are the locations of the integration points on elements i and j, respectively, $|J_{m,n}|$ and $|J_{k,l}|$ are the determinants at the integration points of elements i and j, respectively, W_m, W_n, W_k and W_l are the weighting factors for one-dimensional Gaussian integration. Similarly, the numerical formulas corresponding to Eqs. (24) and (25) are

$$\tilde{e}_Y = \sum_{j=1}^{n} \left\{ \sigma_j \sum_{k=1}^{n_g} \sum_{l=1}^{n_g} \left[G(\xi_{k,l}, \mathbf{Y}) |J_{k,l}| W_k W_l \right] \right\}. \tag{35}$$

and

$$\tilde{\mathbf{I}}_Y = \sum_{j=1}^{n} \left\{ \sigma_j \sum_{k=1}^{n_g} \sum_{l=1}^{n_g} \left[\mathbf{H}(\xi_{k,l}, \mathbf{Y}) \big| J_{k,l} \big| W_k W_l \right] \right\}. \tag{36}$$

Once the distribution of σ_j is computed from Eq. (32), $\tilde{e}_Y$ and $\tilde{\mathbf{I}}_Y$ are computed numerically at any field point from Eqs. (35) and (36).

3.3. Existence and uniqueness problems in the solution

A major drawback in the classical BEM formulation for exterior acoustic radiation and scattering (based on the acoustic pressure and the acoustic velocity on the surface of the model) is that for a discrete set of wave numbers or frequencies (known as irregular frequencies or fictitious frequencies) the solution to the BEM integral equations either does not exist or is not unique [25]. Such an issue does not arise in EBEA. The homogeneous equation corresponding to the EBEA primary system of equations is

$$[K]\{\sigma\} = \{0\}. \tag{37}$$

Along with Eq. (33), it can be observed that the wave number square can be factored out from all the terms and it can be eliminated from the above homogeneous equation. Thus, only the trivial solution can be extracted from the homogeneous equation for non-zero wave numbers. Therefore, the solution of the EBEA is existent and unique for any frequency.

4. Validation of EBEA

In order to demonstrate the validity of the EBEA formulation and its implementation, EBEA results are compared successfully for several analyses to analytical solutions and to numerical results generated by an axi-symmetric *hp* finite-element code with infinite acoustic finite elements. The convergence of the EBEA formulation is also verified.

4.1. Comparison of EBEA with analytical solutions for radiation in an unbounded medium

In order to develop an analytical solution, incoherent point sources are positioned within a radiator. In the analytical solution the surface of the radiator is considered as transparent and the acoustic energy density and acoustic intensity are computed in the field. The normal acoustic intensity on the elements of the transparent surface is also calculated by the analytical solution. The latter comprise the boundary conditions for the EBEA computations. A distribution of acoustic energy sources is evaluated by the EBEA on the surface of the radiator from the intensity boundary conditions which originate from the analytical solution. The surface results of the EBEA computations are employed for calculating the acoustic energy density and the acoustic intensity in the field. Since the incoherent acoustic intensity boundary conditions are the same on the surface of the radiator, both in the analytical solution and the EBEA analysis, it is expected that the field results should correlate between the two methods.

In the analytical solution the expressions for the frequency-averaged acoustic energy density and intensity at any point either on the transparent surface of the radiator, or in the field are, respectively:

$$\tilde{e}_Y = \sum_{i=1}^{m} \left[\bar{\sigma}_i \left(\frac{\rho}{64\pi^2 r_i^4} + \frac{k^2 \rho}{32\pi^2 r_i^2} \right) \right], \tag{38}$$

$$\tilde{\mathbf{I}}_Y = \sum_{i=1}^{m} \left[\bar{\sigma}_i \frac{k^2 \rho c}{32\pi^2 r_i^2} \mathbf{E}_i \right], \tag{39}$$

where m is the number of incoherent point sources that generate the analytical solution, $\bar{\sigma}_i$ is the strength of the ith point source, r_i is the distance between the ith point source and the field point and $\mathbf{E}_i$ indicates the unit vector from the ith point source to the field point. The acoustic power that passes through each element of the transparent surface of the radiator produced by the incoherent point sources is calculated as

$$\bar{P}_i = \int_{S_i} \left\{ \sum_{j=1}^{m} \left[\bar{\sigma}_j \frac{k^2 \rho c}{32\pi^2 r_j^2} \mathbf{E}_j \cdot \mathbf{n}_i \right] \right\} \mathrm{d}S, \quad i = 1, 2, \ldots, n, \tag{40}$$

where $\mathbf{n}_i$ is the unit normal (outward of the structure) vector of element i. In Eqs. (38)–(40) the contribution from each source is added on an energy basis since the individual point sources that create the analytical solution are considered as incoherent with each other.

Results from a cylindrical radiator are compared for three configurations. First, the analytical solution by three incoherent sources located along the axis of the cylinder are developed and compared to the EBEA result. Then, the results from three incoherent sources randomly located off the axis of the cylinder are compared to the EBEA result. Finally, results of the EBEA with different number of elements are compared in order to demonstrate the convergence of the EBEA formulation. The acoustic medium used in the example is water, with density of 1000.0 kg/m^3, and speed of sound equal to 1500.0 m/s. Computations are performed at the center frequency for the 3000 Hz, one-third octave band.

4.1.1. Point sources located along the axis of the cylinder

The geometry of a cylindrical radiator with two end caps is utilized. The radius of the cylinder is 0.5 m, and the length of the cylinder is 10.0 m. The two end caps have the same radius of 0.5 m. The EBEA model for the cylinder is comprised by 376 elements and 378 nodes, and is depicted in Fig. 2. The analytical solution is generated by placing three incoherent point sources of unit strength along the axis of the cylinder (Fig. 3c). The acoustic energy density and the acoustic intensity at any field

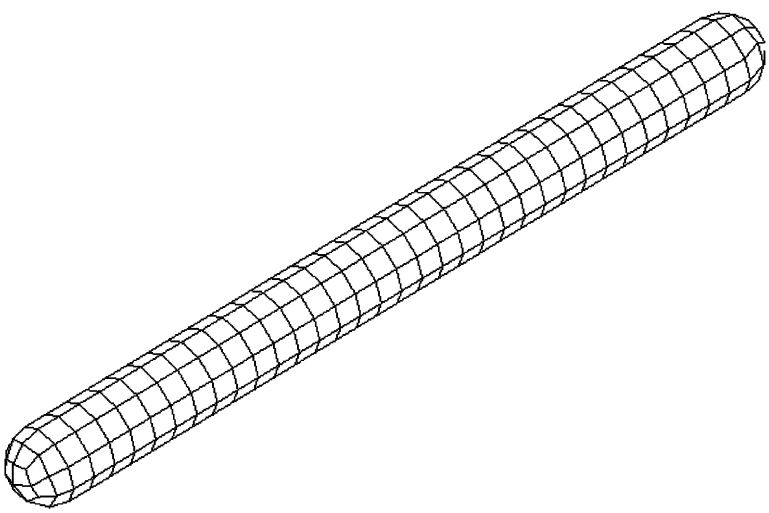

Fig. 2. EBEA model for the cylindrical structure with 376 elements.

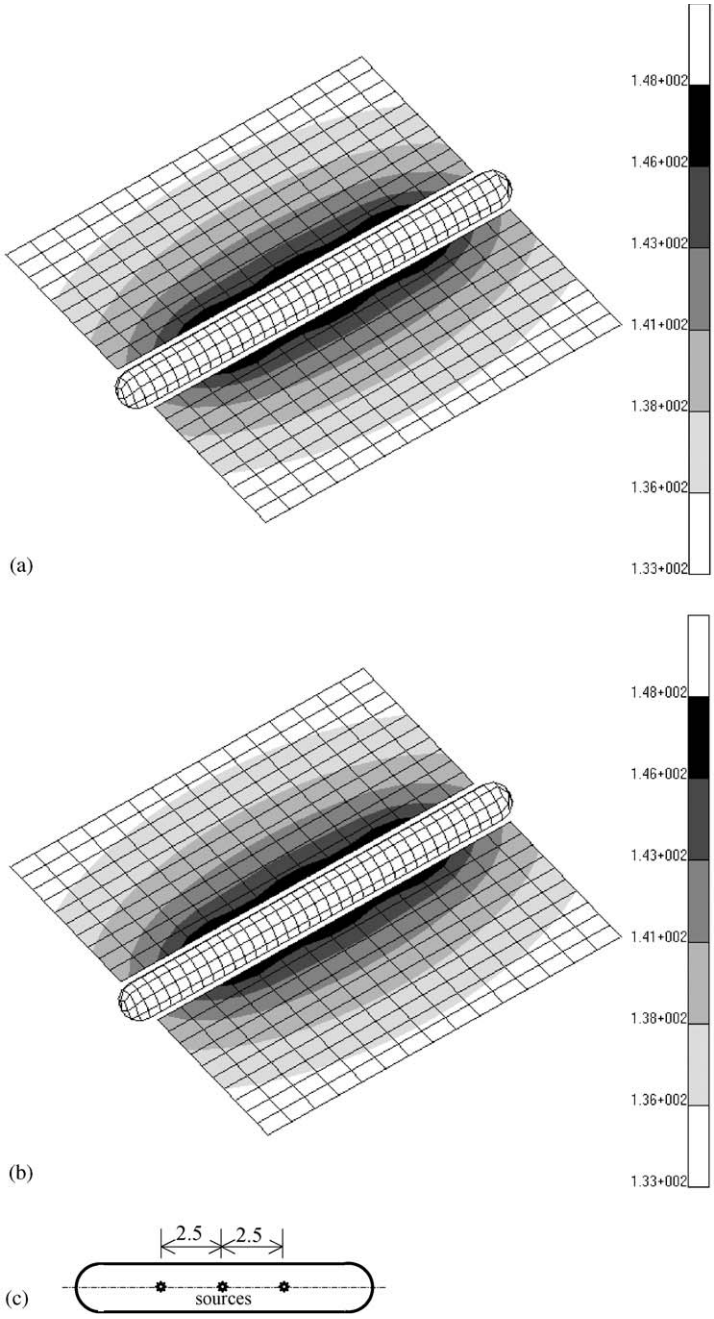

Fig. 3. Distribution of the acoustic energy density (dB, ref. 1e-12) in the field for three incoherent sources located along the axis of the cylinder: (a) the EBEA result, (b) the analytical solution and (c) the sketch of the incoherent sources located along the axis of the cylinder.

point in space are computed analytically using Eqs. (38) and (39), respectively, with $m = 3$. The acoustic normal intensity on each element of the cylindrical surface produced by the three sources is calculated from the analytical solution (Eq. (40)), and constitutes the boundary conditions for the EBEA analysis. The strengths of the acoustic energy sources distributed over the surface of the cylindrical radiator are calculated by the EBEA and used in the field computations. The contours of the acoustic energy density in the field computed by the EBEA and by the analytical solution are depicted in Fig. 3(a) and (b), respectively. The vector distributions of the acoustic intensity in the field obtained from the EBEA and from the analytical method appear in Fig. 4(a) and (b), respectively. The analytical and the EBEA results correlate very well for both the far field and near field. The EBEA captures the symmetric characteristics of the near field response properly.

4.1.2. Point sources located off the axis of the cylinder

The same cylindrical radiator is analyzed again, but this time the three incoherent sources are placed off the axis of the cylinder as depicted in Fig. 5c. The analytical solutions for the acoustic energy density and the acoustic intensity in the field are computed using Eqs. (38) and (39), respectively, with $m = 3$. The boundary conditions for the EBEA analysis are calculated by Eq. (40). The contours of the acoustic energy density in the field computed by the EBEA and by the analytical solution are depicted in Fig. 5(a) and (b), respectively. The vector distributions of the acoustic intensity in the field obtained from the EBEA and from the analytical method appear in Fig. 6(a) and (b), respectively. Again, when the incoherent sources are located off the axis of the cylinder, the analytical and the EBEA results correlate very well. The EBEA captures correctly the characteristics of the acoustic field in the vicinity of the radiator. In order to demonstrate the difference between the EBEA compared with modelling the radiator as a single point source with power equal to the total power of all the incoherent sources, a single point source located at the center of the cylinder is used to approximate the cylindrical radiator. The strength of this single point source is determined by equating the total radiated acoustic power to that from the three point

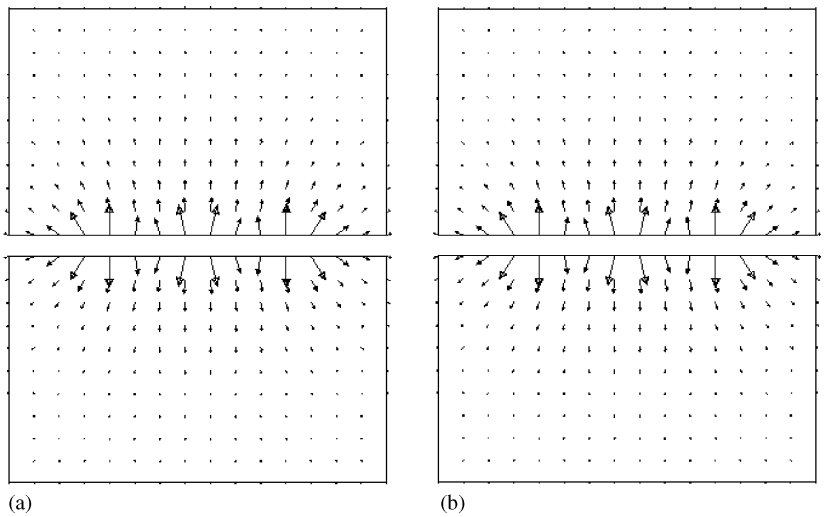

Fig. 4. Distribution of the acoustic intensity vector in the field for three incoherent sources located along the axis of the cylinder: (a) the EBEA result and (b) the analytical solution.

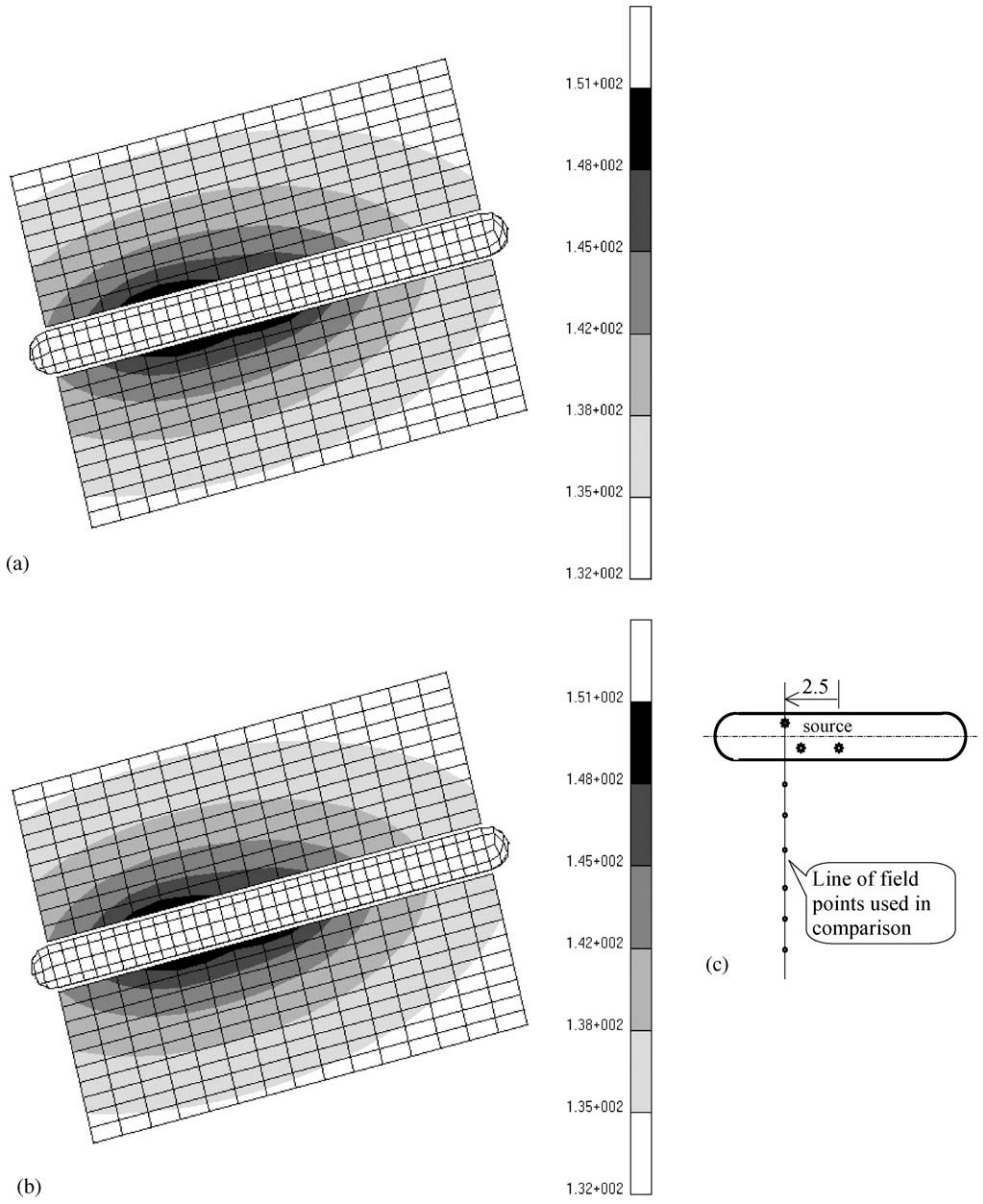

Fig. 5. Distribution of the acoustic energy density (dB, ref. 1e-12) in the field for three incoherent sources placed off the axis of the cylinder: (a) the EBEA result, (b) the analytical solution and (c) the sketch of the incoherent sources located off the axis of the cylinder.

sources used in the example. Acoustic energy densities at field points placed 1 m apart along a line defined in Fig. 5c are presented in Fig. 7 for comparison. As expected, for field points several diameters away from the cylinder both the EBEA and the single point source approximation give almost the same results. However, in the vicinity of the radiator, the EBEA provides much better correlation with the analytical solution than the single source approximation.

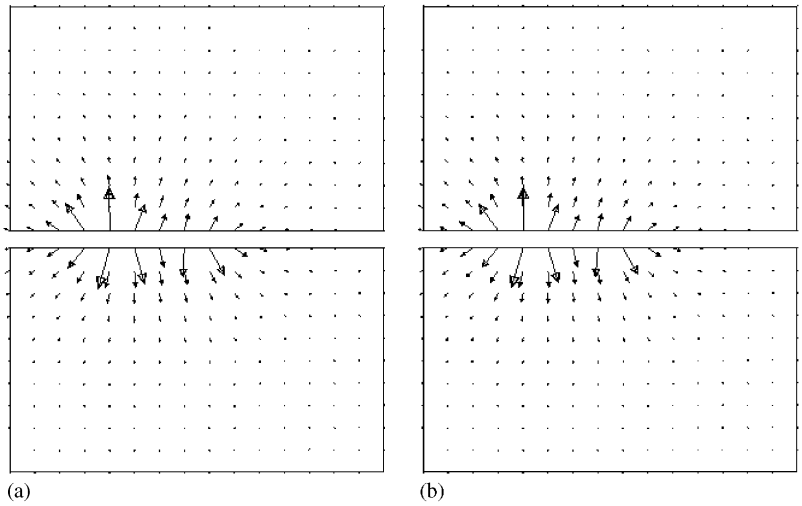

Fig. 6. Distribution of the acoustic intensity vector in the field for three incoherent sources placed off the axis of the cylinder: (a) the EBEA result and (b) the analytical solution.

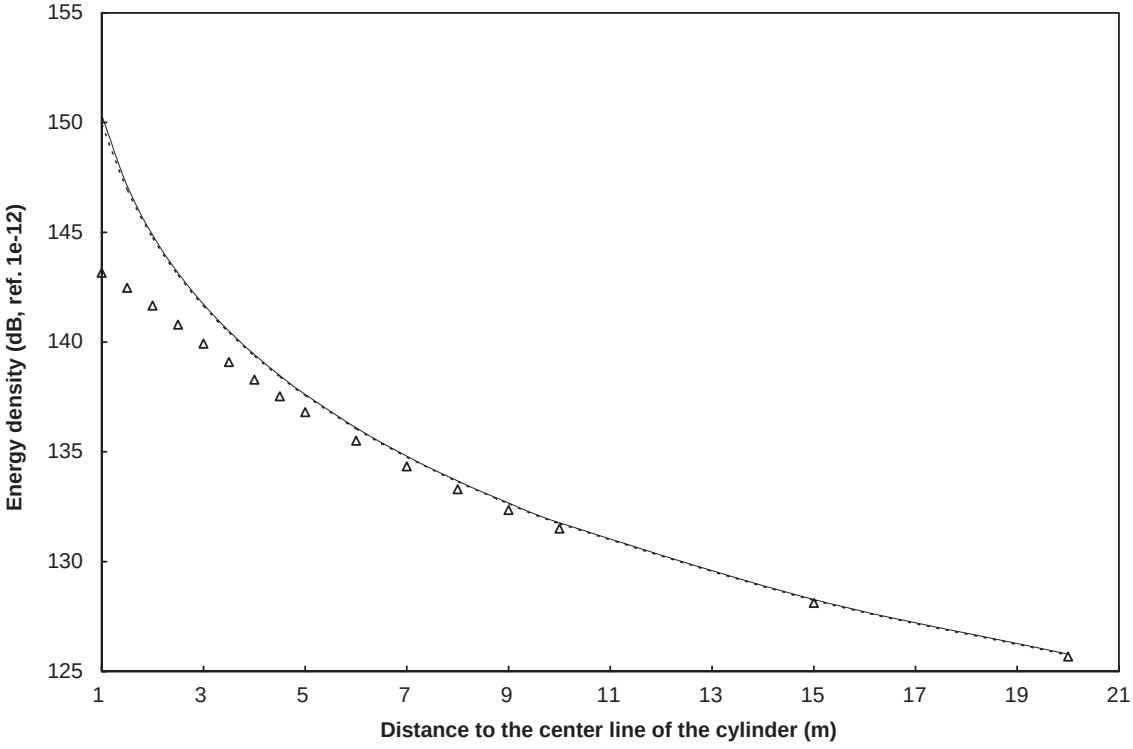

Fig. 7. Comparison of the acoustic energy density among the EBEA, the analytical solution and the single source approximation (dB, ref. 1e-12): ——, EBEA; - - - -, analytical solution; △, single source approximation.

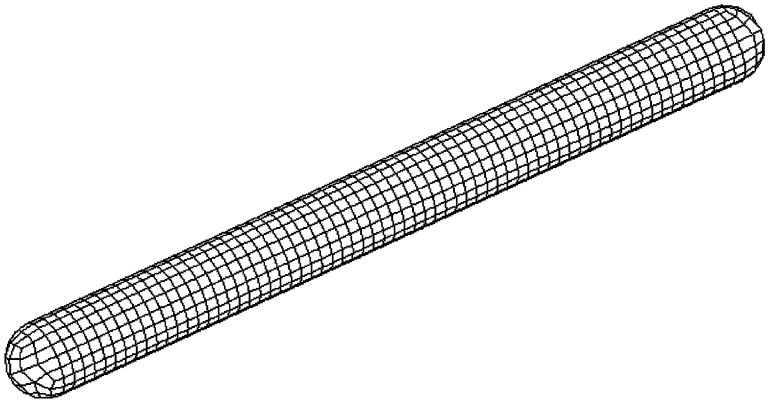

Fig. 8. EBEA model of the cylindrical structure with 1437 elements.

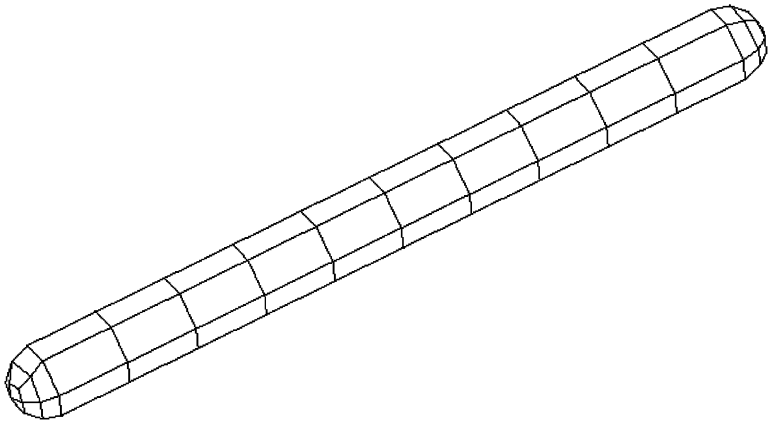

Fig. 9. EBEA model of the cylindrical structure with 92 elements.

4.1.3. Convergence of the EBEA formulations

In order to verify the convergence of the EBEA formulation, the same cylindrical radiator is discretized by different number of boundary elements. The results corresponding to the three incoherent sources placed along the axis of the cylinder are used to compare the results from the models comprised by different number of elements. Three models with different element densities are used, the original model presented in Fig. 2, a model with more elements (1437 elements and 1439 nodes) is presented in Fig. 8, and a model with less elements (92 elements and 94 nodes) is presented in Fig. 9.

The acoustic energy density and the magnitude of the acoustic intensity at field points placed at various distances from the center of the cylinder within the $X-Y$ plane are presented in Figs. 10 and 11, respectively. Overall, good correlation is observed between the analytical solution and the EBEA results for both the acoustic energy density and the acoustic intensity magnitude in the field. It can be observed that the correlation can be improved and the EBEA results converge to the analytical solution as the number of elements in the model increases.

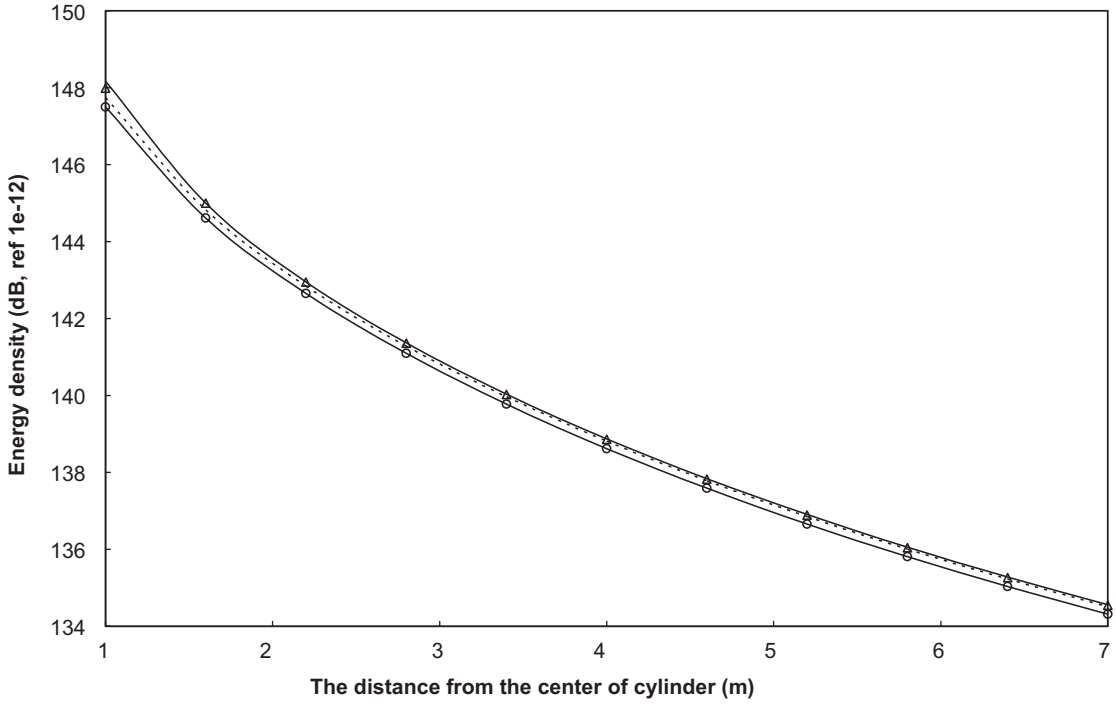

Fig. 10. Comparison of the acoustic energy density (dB, ref. 1e-12): ——, EBEA with 376 elements; △, EBEA with 1437 elements; -o-, EBEA with 92 elements; - - - -, analytical solution.

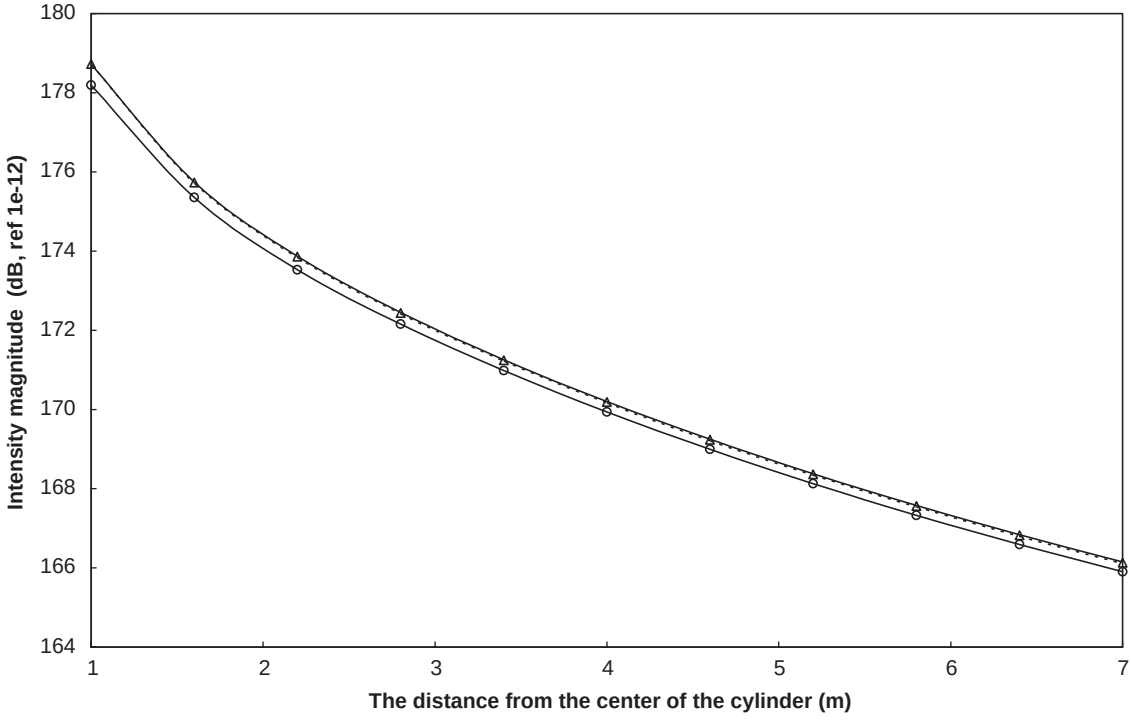

Fig. 11. Comparison of the acoustic intensity magnitude (dB, ref. 1e-12): ——, EBEA with 376 elements; △, EBEA with 1437 elements; -o-, EBEA with 92 elements; - - - -, analytical solution.

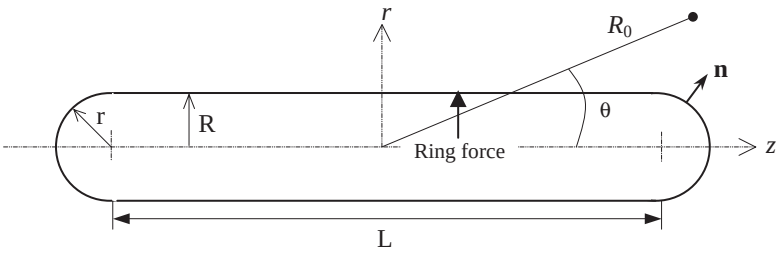

Fig. 12. Dimensions of the cylinder with spherical end-caps.

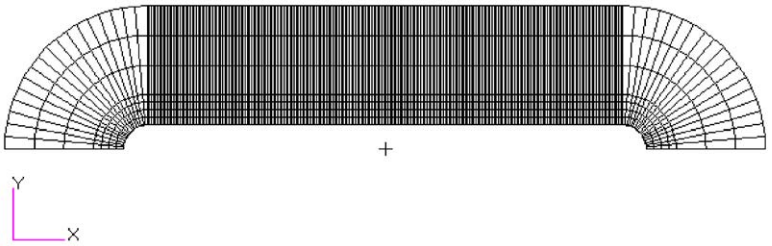

Fig. 13. Mesh of the cylinder with end-caps for the SONAX model.

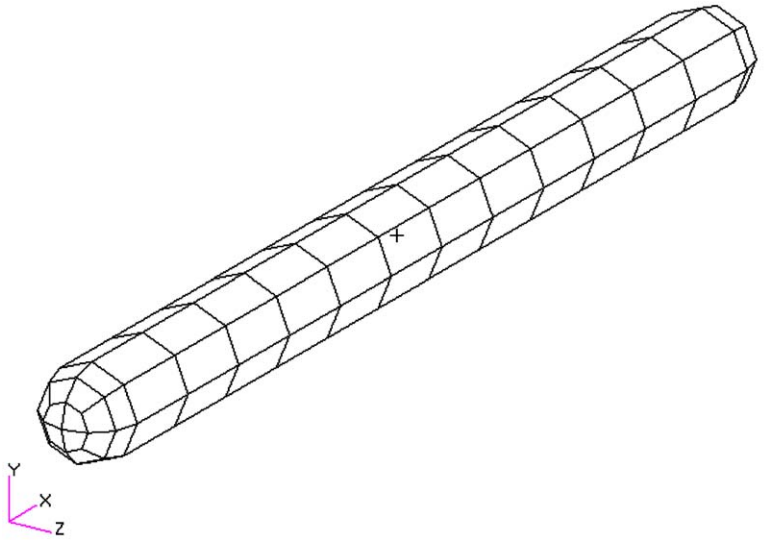

Fig. 14. Mesh of the cylinder with end-caps for the EBEA model.

4.2. Comparison between EBEA and infinite finite elements for radiation analysis

In this validation an axi-symmetric *hp* finite-element code with infinite acoustic finite elements (SONAX) [32] is utilized. SONAX can model both a vibrating structure and the acoustic radiation in the surrounding medium. SONAX is used for generating the normal acoustic intensity boundary conditions for the EBEA analysis, and for computing acoustic results in the field. The latter are used as a basis for comparison with the EBEA results. The vibration and the corresponding acoustic

radiation from an axi-symmetric structure are analyzed in this validation. Analyses are performed within an intermediate frequency range where both solutions (SONAX and EBEA) are expected to be valid. A cylindrical structure depicted in Fig. 12 is analyzed. The radius of the cylinder is $R = 0.3$ m, while the length is $L = 6.0$ m, and the thickness is equal to 0.005 m. The two spherical end-caps have the same radius $r = 0.3$ m, and thickness of 0.005 m. The material properties of the structure are: Young's modulus $E = 2.0 \times 10^{11}$ Pa, Poisson's ratio $v = 0.28$, density $\rho_s = 7800.0\,\mathrm{kg/m^3}$, damping factor $\eta_s = 0.02$. The exterior acoustic medium is water ($\rho_f = 1000.0\,\mathrm{kg/m^3}$, $c = 1500.0$ m/s). The SONAX finite-element model for the structure and the surrounding medium are depicted in Fig. 13. A large number of finite elements are used in the axi-symmetric model in order for the results to be valid at a high-frequency range for a meaningful comparison with the EBEA. A ring force of unit strength is applied at $z = 1.0$ m on the structure and SONAX is used for calculating the surface vibration, the surface acoustic pressure, and the farfield acoustic pressure. Analyses are performed at 5 Hz intervals within the 1600 and 2000 Hz one-third octave frequency bands and all of the SONAX results are frequency-averaged within each band. The surface vibration and the surface acoustic pressure are employed for calculating the frequency-averaged acoustic normal intensity on the surface of the cylinder. The latter is employed for defining the boundary conditions for the EBEA analysis. The results for the farfield frequency-averaged acoustic intensity computed by SONAX and by the EBEA are compared. The EBEA model employed in the computations is depicted in Fig. 14.

The equations utilized for processing the SONAX results in order to generate the boundary conditions for the EBEA analysis are presented. The complex acoustic pressure and normal displacement (outward of the cylinder) on the surface of the structure are computed by SONAX at each node of the axi-symmetric finite-element model and for each frequency of analysis:

$$\hat{p} = p_r + \mathrm{i}p_i, \quad \hat{d}^n = d_r^n + \mathrm{i}d_i^n, \tag{41,42}$$

where p_r and p_i represent the real and imaginary parts of the complex acoustic pressure respectively, and d_r^n and d_i^n are the real and imaginary parts of the complex normal displacement. Considering harmonic vibration, the normal acoustic velocity on the surface of the structure can be written as [9,35]

$$v_n = \frac{\mathrm{d}}{\mathrm{d}t}(d^n) = (\omega d_i^n - \mathrm{i}\omega d_r^n)\mathrm{e}^{-\mathrm{i}\omega t} \text{ or } \hat{v}_n = \omega d_i^n - \mathrm{i}\omega d_r^n. \tag{43}$$

According to Eq. (6), the time-averaged normal acoustic intensity on the surface of the cylinder and at each node of the axi-symmetric model is equal to

$$\langle I \rangle_n = \tfrac{1}{2}\omega(p_r d_i^n - p_i d_r^n). \tag{44}$$

The results for the time-averaged normal acoustic intensity are processed in order to generate the appropriate intensity boundary conditions for the EBEA analyses. First, the results from Eq. (44) are frequency-averaged over the one-third octave band where analyses are performed. Since the elements in the SONAX model are considerably smaller than the elements in the EBEA model, the time and frequency-averaged normal acoustic intensity from SONAX is further integrated over each EBEA element. These integrated values on every EBEA element define the boundary conditions for the EBEA analyses. The farfield acoustic pressure $\hat{p}_{R_0}$ is also computed by SONAX. By considering a plane wave assumption for the farfield acoustic response the

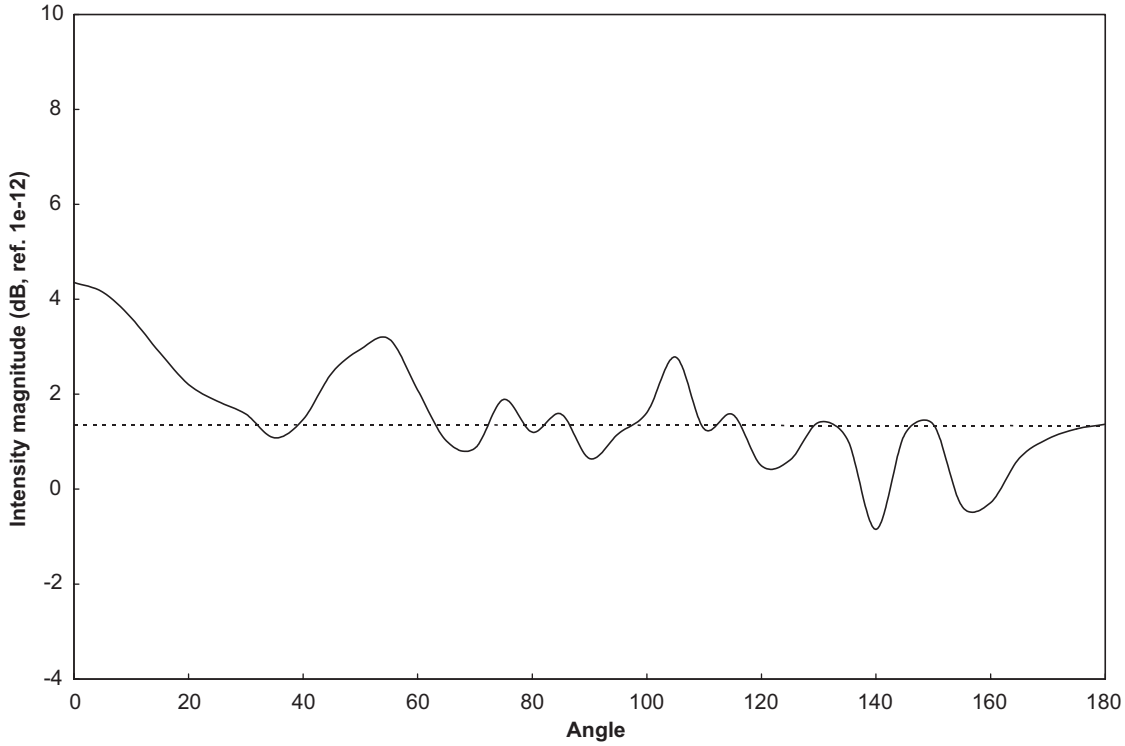

Fig. 15. Time and frequency-averaged farfield acoustic intensity magnitude (dB, ref. 1e-12) at $R_0 = 1000$ m with the central frequency of 1600 Hz: - - - - -, EBEA; ——, the analytical solution.

magnitude of the corresponding time-averaged acoustic intensity is equal to

$$\langle I \rangle_{R_0} = \frac{|\hat{p}_{R_0}|^2}{2\rho c}. \tag{45}$$

In order to compare the time-averaged acoustic intensity computed by SONAX in the far field with the EBEA results, the acoustic intensity from Eq. (45) is frequency-averaged over the two one-third octave bands where analyses are performed.

In the EBEA analysis, the time and frequency-averaged normal acoustic intensity evaluated on the surface of the EBEA model from the SONAX results comprises the boundary conditions. The distribution of the acoustic energy sources on the surface of the EBEA model is computed first and then the time and frequency-averaged acoustic energy density and intensity in the field are evaluated from Eqs. (24) and (25). Results in the far field are computed by both methods for a radius $R_0 = 1000$ m, and for multiple polar angles. Results for the magnitude of the acoustic intensity (dB) calculated by SONAX and by the EBEA for 1600 and 2000 Hz one-third octave bands are depicted in Figs. 15 and 16, respectively. The horizontal axis represents the polar angle θ (degree) as defined in Fig. 12. Good correlation is observed in the results. Variation of the acoustic intensity with respect to the polar angle is not present in the EBEA results due to the space averaging that is performed in order to generate the EBEA boundary conditions from

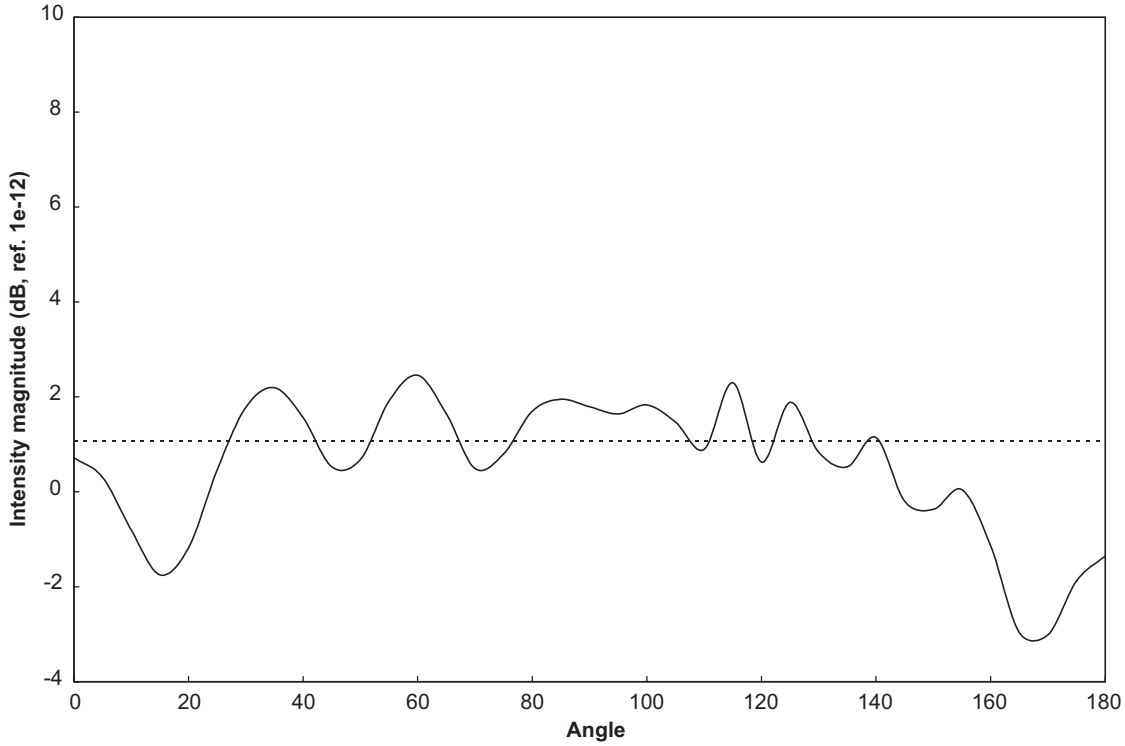

Fig. 16. Time and frequency-averaged farfield acoustic intensity magnitude (dB, ref. 1e-12) at $R_0 = 1000\,\text{m}$ with the central frequency of 2000 Hz: ----, EBEA; ——, the analytical solution.

the SONAX results, and due to the consideration of the distributed energy sources as incoherent in the EBEA formulation.

5. Conclusions

An energy boundary element analysis (EBEA) formulation for acoustic radiation in an unbound fluid with no dissipation and its numerical implementation are presented. The EBEA can be employed for calculating the acoustic field generated at high frequency from a radiator on which incoherent intensity boundary conditions are defined. In practical applications the intensity boundary conditions originate from an EFEA analysis which computes the structural vibration of a structure surrounding by a fluid and the corresponding radiated power [33]. The EBEA presented in this paper completes a void exhibited by the high-frequency methods of SEA and EFEA in modelling radiation in an unbound medium. The SEA and the EFEA can model enclosed acoustic spaces but they require definition of damping properties and the existence of an orthogonal modal or wave basis (i.e., assumption of reverberant field) for modelling an acoustic space. Thus, neither method is suitable for modelling radiation in an unbound medium. Previous EBEA formulations concentrated in solving interior acoustic applications where damping is

considered for the acoustic meidum. The EBEA presented in this paper does not require to define damping properties for the infinite fluid and no assumptions are made about representing the unbounded acoustic medium as reverberant. Good correlation is demonstrated between the EBEA results and analytical or infinite finite element solutions for several analyses of acoustic radiation. The EBEA computes better results for the acoustic field in the vicinity of the radiator compared to a simplified and approximate solution produced by a single source placed at the center of the radiator and with power equal to the total power of the radiator.

Acknowledgements

The research presented in this paper was supported by the Office of Naval Research, Code 334, under contract no. N00014-00-1-0382. The authors acknowledge Dr. Luise Couchman and Mr. Terry Bazow for their assistance in utilizing the SONAX code.

References

[1] R.J. Berhard, J.E. Huff, Structure-acoustic design at high frequency using the energy finite element method, *Journal of Vibration and Acoustics* 121 (1999) 295–301.
[2] N. Vlahopoulos, O.G. Luis, M. Christopher, Numerical implementation validation and marine applications of an energy finite element formulation, *Journal of Ship Research* 43 (1999) 143–156.
[3] W. Zhang, A. Wang, N. Vlahopoulos, An alternative energy finite element formulation based on incoherent orthogonal waves and its validation for marine structures, *Finite Elements in Analysis and Design* 38 (2002) 1095–1113.
[4] W. Zhang, A. Wang, N. Vlahopoulos, Validation of the EFEA method through correlation with conventional FEA and SEA results, *Proceedings of the 2001 SAE Noise and Vibration Conference*, SAE paper 2001-01-1618, 2001.
[5] N. Vlahopoulos, X. Zhao, An investigation of power flow in the mid-frequency range for systems of co-linear beams based on a hybrid finite element formulation, *Journal of Sound and Vibration* 242 (2001) 445–473.
[6] O.M. Bouthier, R.J. Bernhard, Models of space-averaged energetics of plates, *American Institute of Aeronautics and Astronautics Journal* 30 (1992) 34–44.
[7] O.M. Bouthier, Energetics of Vibrating Systems, PhD Dissertation, Mechanical Engineering Department, Purdue University, Lafayette, IN, 1992.
[8] R. Lyon, *Statistical Energy Analysis of Dynamical Systems: Theory and Application,*, MIT Press, Cambridge, MA, 1975.
[9] L. Cremer, M. Heckl, E.E. Ungar, *Structure-Born Sound*, Springer, Berlin, 1973.
[10] A. Le Bot, L. Ricol, Integral equation instead of heat conduction equation for medium and high frequencies, in: *Inter-Noise*, 1995, pp. 579–582.
[11] F. Bitsie, R.J. Bernhard, The structural–acoustic energy finite element method and energy boundary element method, Internal Report #209, Ray W. Herrick Laboratories, Purdue University, West Lafayette, IN, 1996.
[12] S.T. Raveendra, J.K. Thompson, C.M. Mollo, Boundary element method for high frequency acoustic analysis, in: *Proceedings of the ASME Noise Control and Acoustic Division*, 1997, pp. 309–313.
[13] F. Thouverez, M. Viktorovitch, L. Jezequel, A random boundary element formulation for assembled rods and beams in the mid frequency range, in: L. Jezequel (Ed.), *New Advances in Modal Synthesis of Large Structures: Non-linear Damped and Non-deterministic Cases*, Balkema, Rotterdam, 1997, pp. 435–444.
[14] A. Le Bot, A vibroacoustic model for high frequency analysis, *Journal of Sound and Vibration* 211 (1998) 537–554.
[15] L.H. Chen, D.G. Schweikert, Sound radiation from an arbitrary body, *Journal of the Acoustical Society of America* 35 (1963) 1626–1632.

[16] C.A. Brebbia, J.C. Telles, L.C. Wrobel, *Boundary Element Techniques*, Springer, Berlin, 1984.
[17] G. Chertock, Sound radiation from vibrating surfaces, *Journal of the Acoustical Society of America* 36 (1964) 1305–1313.
[18] L.C. Copley, Integral equation method for radiation from vibrating bodies, *Journal of the Acoustical Society of America* 41 (1967) 807–816.
[19] H.A. Schenck, Improved integral formulation for acoustic radiation problems, *Journal of the Acoustical Society of America* 44 (1968) 41–58.
[20] A.F. Seybert, T.K. Rengarajan, The use of CHIEF to obtain unique solutions for solutions for acoustic radiation using boundary integral equations, *Journal of the Acoustical Society of America* 81 (1987) 1299–1306.
[21] A.J. Burton, G.F. Miller, The application of the integral equation method to the numerical solution of some exterior boundary value problems, *Proceedings of the Royal Society of London* 323 (1971) 201–210.
[22] M. Ochmann, The full-field equations for acoustic radiation and scattering, *Journal of the Acoustical Society of America* 105 (1999) 2574–2584.
[23] L. Bouchet, T. Loyau, N. Hamzaoui, C. Boisson, Calculation of acoustic radiation using equivalent-sphere methods, *Journal of the Acoustical Society of America* 107 (2000) 2387–2397.
[24] A.F. Seybert, B. Soenarko, D.J. Shippy, An advanced computational method for radiation and scattering of acoustic waves in three dimensions, *Journal of the Acoustical Society of America* 77 (1985) 362–368.
[25] G.W. Benthien, H.A. Schenck, Nonexistence and nonuniqueness problems associated with integral equation method in acoustic, *Computers & Structures* 65 (1997) 295–305.
[26] R.K. Andrew, R.L. Kirlin, A broadband maximum likelihood imager for a class of extended space-time separable sources, *IEEE Transactions on Signal Processing* 48 (2000) 1287–1294.
[27] J. Li, J. Pascal, Energy fields of partially coherent sources, *Journal of the Acoustical Society of America* 103 (1998) 962–972.
[28] B.R. Mace, Power flow between two coupled beams, *Journal of Sound and Vibration* 159 (1992) 495–529.
[29] A.J. Keane, A note on modal summations and averaging methods as applied to statistical energy analysis (SEA), *Journal of Sound and Vibration* 164 (1993) 143–156.
[30] E.C.N. Wester, B.R. Mace, Statistical energy analysis of two edge-coupled rectangular plates: ensemble averages, *Journal of Sound and Vibration* 193 (1996) 793–822.
[31] J.L. Hess, A.M.O. Smith, in: *Progress in Aeronautical Sciences, D. Calculation of Potential Flows about Arbitrary Bodies*, Vol. 8, Pergamon Press, New York, 1967.
[32] T. Bazow, *SONAX User's Manual*, Naval Research Laboratory, Washington, DC, 1997.
[33] W. Zhang, A. Wang, N. Vlahapoulos, K. Wu, High-frequency vibration analysis of thin elastic plates under heavy fluid loading by an energy finite element formulation, *Journal of Sound and Vibration* 263 (2003) 21–46.
[34] A.D. Pierce, *Acoustics: An Introduction to its Physical Principles and Applications*, McGraw-Hill Press, New York, 1981.
[35] M.C. Junger, D. Feit, *Sound Structures and their Interaction*, MIT Press, Cambridge, MA, 1993.